Harmonic behavior of the multiple quantum resonances of a two-level atom driven by a fully-amplitude-modulated field

Wilhelmus M. Ruyten
Center for Laser Applications, University of Tennessee Space Institute, Tullahoma, Tennessee 37388
(Received 17 March 1989)

We present a detailed theoretical treatment of the response of a two-level atom to a fully-amplitude-modulated, narrow-band optical field. Specifically, we calculate the resonance behavior of modulated fluorescence and susceptibility components from the scalar continued-fraction solution of the optical Bloch equations. In the limit of vanishing damping the resonances are generally doubly branched: One set of branches reproduces the resonances of the time-averaged fluorescence, while the second set is different for each harmonic component. However, each branch is uniquely associated with an odd multiple quantum resonance. In analogy with magnetic resonance work, we derive analytical expressions for the generalized Bloch-Siegert shifts of the additional resonances. We discuss also the possibility of experimental verification of the theory.

I. INTRODUCTION

One of the successful testing grounds for the theory of matter-radiation interaction has been in the area of magnetic resonance. In a much studied geometry a spin-$\frac{1}{2}$ atom is subjected to a static Zeeman field $\mathbf{H}_0$ and a radio-frequency (rf) field perpendicular to $\mathbf{H}_0$. The longitudinal pumping configuration, in which a population difference between the Zeeman-split levels is induced by circularly polarized light propagating along $\mathbf{H}_0$, is well known for its multiple quantum resonances.[1] For small amplitudes of the rf field these resonances occur when the Rabi frequency, associated with $\mathbf{H}_0$, equals an odd multiple of the rf frequency. As the rf amplitude increases the resonances undergo the well-known Bloch-Siegert shift and disappear for sufficiently strong rf fields.

In 1972 Stenholm showed that the solution of the pertinent Bloch equations can be obtained in terms of scalar continued fractions, valid for arbitrary rf amplitudes.[2] Unlike Shirley's earlier characteristic exponent method, which is based on diagonalization of the Floquet Hamiltonian, and does not include relaxation effects,[3] Stenholm's theory not only gives the solution for the time-averaged (dc) behavior, but for modulated interaction components as well. However, expressions for the Bloch-Siegert shifts of the multiple-quantum resonances, derived from Stenholm's theory[2,4] or otherwise,[5,6] have been calculated for the dc fluorescence and absorption components only. This is surprising because, concurrent with the development of the theory, experimental work was performed in which modulated signals rather than dc signals were measured.[7] In their brief theoretical treatment, Arimondo and Moruzzi conclude that " ... the same Bloch-Siegert shift is displayed by both the stationary term and the time-dependent term (at twice the modulation frequency) at low intensities of the rf field ..., " but that " ... on the contrary, a different behavior is observed at higher fields ... ."[7] Thus, although it was recognized that the resonance behavior of modulated interaction components deviates from that of the dc behavior in general, no detailed analysis was performed.

By now, interest in the above type of magnetic resonance experiments has largely subsided. However, a mathematically identical problem has emerged in the field of optical resonance, namely, the interaction of a fully-amplitude-modulated (FAM), narrow-band laser with an optical two-level atom. Here the detuning and the electric dipole coupling replace the roles of the Zeeman splitting and the magnetic dipole coupling, respectively. Again the system is easily shown to possess multiple quantum resonances (Fig. 1). In 1976 Feneuille *et al.* solved the problem for strong, resonant excitation.[8] At about the same time Thomann performed both theoretical and experimental work for a not-fully-amplitude-modulated laser.[9] Then in 1984 Hillman *et al.* showed that the theory of a FAM interaction successfully describes the bichromatic operation of a homogeneously broadened laser.[10] However, not until 1988 did Chakmakjian *et al.* report experimental results for a FAM interaction in which multiple quantum resonances were directly observed,[11] namely, as subharmonic resonances in the dc fluorescence signal from a beam of sodium atoms.[12]

Conceivably, an experiment like that of Chakmakjian *et al.* could be performed, in which not the dc fluorescence but the modulated components of the fluorescence would be detected. In fact, measurement of the fluorescence at the beat frequency of a modulated driving field forms the basis for many fluorometric techniques, and accounts for our interest in the subject.[13] Thus we investigate the influence of multiple quantum resonances on the harmonic behavior of a two-level system, driven by a FAM field. In the following we assume an optical resonance experiment—the treatment for a longitudinally pumped magnetic rf experiment would be identical.

In Sec. II we review Stenholm's continued-fraction solution and the Bessel-function solution for zero detuning. To illustrate the resonance behavior of harmonic

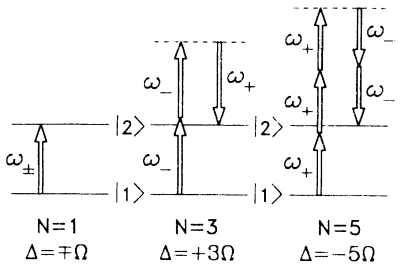

FIG. 1. Illustration of multiple quantum resonances in a two-level atom. ω_+ and ω_- denote up- and down-shifted photons of the fully-amplitude-modulated (bichromatic) field. In the weak-field limit resonances occur when the detuning Δ equals an odd multiple N of the modulation frequency Ω.

components we compute results for the dc fluorescence and the lowest fluorescence harmonic, and show that the corresponding multiple quantum resonances are singly and doubly branched, respectively.[14] In Sec. III we take the vanishing damping limit of the continued-fraction solution and generalize the Bessel-function result from Sec. II. In passing we show that, in the vanishing damping limit, a dc population inversion of the two-level system is impossible. Using the solution from Sec. III we derive in Sec. IV the doubly branched structure of the multiple quantum resonances explicitly, and calculate expressions for the generalized Bloch-Siegert shifts of *all* harmonics. Finally, in Sec. V we conclude with a discussion on practical implications and possible experimental verification of the theory.

II. GENERAL SOLUTION

Following the notation of Allen and Eberly[15] we write the optical Bloch equations for a two-level atom interacting with an electric field of amplitude $\mathcal{E}(t)$ as

$$\dot{U} = -U/T_2 - \Delta V \ , \tag{2.1a}$$

$$\dot{V} = \Delta U - V/T_2 + \kappa \mathcal{E}(t) W \ , \tag{2.1b}$$

$$\dot{W} = -(W - W_{\rm eq})/T_1 - \kappa \mathcal{E}(t) V \ , \tag{2.1c}$$

where Δ is the detuning, κ is the dipole-coupling constant, $W_{\rm eq}$ is the equilibrium inversion, and T_1 and T_2 are the longitudinal and transverse relaxation times. Assuming that the field is fully amplitude modulated at frequency Ω, we write the time-dependent Rabi frequency as

$$\kappa \mathcal{E}(t) = 2g \cos \Omega t \ . \tag{2.2}$$

Below we refer to the constant g simply as "the Rabi frequency." To allow for unequal damping rates for the susceptibility components U and V (as is generally the case in the equivalent magnetic resonance geometry) we replace the damping rates $1/T_2$, $1/T_2$, and $1/T_1$ in Eqs. (2.1) by Γ_u, Γ_v, and Γ_w, respectively. Also, we choose alternative definitions for the components of the Bloch vector, for ease of notation below:[16]

$$u = -U, \quad v = -iV, \quad w = -W \ . \tag{2.3}$$

Thus v corresponds to the difference between (rather than the imaginary part of) the rotating-frame off-diagonal density-matrix elements, and an inverted system is characterized by values $w < 0$. Finally, because the solution of Eqs. (2.1) scales linearly with $W_{\rm eq}$ we assume—without loss of generality—that $W_{\rm eq} = -1$. The Bloch equations from Eqs. (2.1) now become

$$\dot{u} + \Gamma_u u = i \Delta v \ , \tag{2.4a}$$

$$\dot{v} + \Gamma_v v = i \Delta u + 2igw \cos \Omega t \ , \tag{2.4b}$$

$$\dot{w} + \Gamma_w w = 2igv \cos \Omega t + \Gamma_w \ . \tag{2.4c}$$

By the Floquet theorem the steady-state solution of Eqs. (2.4) can be written as

$$z(t) = \sum_{k=-\infty}^{\infty} z_k \exp(ik\Omega t) \ , \quad z = u, v, w \ . \tag{2.5}$$

Substitution of Eq. (2.5) into Eqs. (2.4) yields a set of recurrence relations between the Floquet coefficients. As was first shown by Stenholm these recurrence relations can be solved in terms of scalar continued fractions.[2,17] Specifically, because even terms v_k and odd terms w_k vanish, and because the u_k's follow simply from the v_k's by

$$u_k = i \Delta v_k / (\Gamma_u + ik\Omega) \ , \tag{2.6}$$

it suffices to solve for the combined coefficients

$$\psi_k = \begin{cases} v_k, & k = \text{odd} \\ w_k, & k = \text{even} \end{cases} \ . \tag{2.7}$$

Thus Eqs. (2.4) can be reduced to a single, three-term recurrence relation

$$a_k \psi_k - ig(\psi_{k-1} + \psi_{k+1}) = \Gamma_w \delta_{k,0} \ ,$$

where

$$a_k = \begin{cases} \Gamma_v + ik\Omega + \dfrac{\Delta^2}{\Gamma_u + ik\Omega}, & k = \text{odd} \\ \Gamma_w + ik\Omega, & k = \text{even} \end{cases} \ . \tag{2.8}$$

From this recurrence relation the quantities x_k, defined as $x_k = \psi_k / \psi_{k-1}$, can be obtained as continued fractions by backward iteration of

$$x_k = (a_k/ig - x_{k+1})^{-1}, \quad k \geq 1 \ . \tag{2.9}$$

For accurate results the backward iteration should be started at a value of k no smaller than $(\Delta^2 + 4g^2)^{1/2}$. For $k \leq 0$ it can be shown that $x_k^{-1} = -x_{1-k}^*$. Thus the solution for the dc component becomes

$$\psi_0=[1+2g\ \mathrm{Im}(x_1)/\Gamma_w]^{-1}\ . \tag{2.10}$$

Once the x_k's and ψ_0 have been determined, the harmonic components are obtained by forward recursion:

$$\psi_k=x_k\psi_{k-1},\quad k\geq 1\ . \tag{2.11}$$

For negative indices one finds

$$\psi_k=(-1)^k\psi^*_{-k},\quad k\leq 0\ , \tag{2.12}$$

which follows also from the fact that $v(t)$ and $w(t)$ are imaginary and real, respectively. With Eqs. (2.5)–(2.12) the steady-state solution of Eqs. (2.4) is completely determined.

For the special case $\Delta=0$ and equal damping rates, i.e., $\Gamma_v=\Gamma_w$, Eqs. (2.4) can be solved analytically in terms of integer-order Bessel functions.[2–6,8] If the results for $v(t)$ and $w(t)$ are expanded as a Floquet series as in Eq. (2.5), and the coefficients from Eq. (2.7) are denoted by ϕ_k, i.e.,

$$\phi_k\equiv\psi_k(\Delta=0;\ \Gamma_v=\Gamma_w)\ , \tag{2.13}$$

one obtains

$$\phi_k=\sum_{l=-\infty}^{\infty}\frac{J_l(2g/\Omega)J_{k+l}(2g/\Omega)}{1-il\Omega/\Gamma_w}\ . \tag{2.14}$$

In the limit of vanishing damping only one term out of the infinite sum from Eq. (2.14) contributes, yielding the simple result

$$\phi_k^0\equiv\lim_{\Gamma_w\to 0}\phi_k=J_0(2g/\Omega)J_k(2g/\Omega)\ . \tag{2.15}$$

Equation (2.15) provides an important clue about the resonance behavior of harmonic components of the interaction. That is, for $k\neq 0$, ϕ_k^0 shares one set of zeros with the dc term ϕ_0^0, namely, those of $J_0(2g/\Omega)$, but also contains an extra set of zeros, namely, those of $J_k(2g/\Omega)$.

To illustrate the resonance behavior of the system we have computed the dc fluorescence component $(1-\psi_0)/2$ and the amplitude $|\psi_2|$ of the lowest fluorescence harmonic using the continued-fraction solution of Eqs. (2.8)–(2.11). The results are displayed in Fig. 2 as a function of the scaled detuning Δ/Ω for a fixed interaction strength, namely, $\Gamma/w=4$. Different curves correspond to different values of the damping—it has been assumed that $\Gamma_u=\Gamma_v=\Gamma_w$. The solid curves are for a vanishingly small damping, namely, $\Gamma_w/\Omega=10^{-8}$. Their limiting values for $\Delta=0$ are correctly given by Eq. (2.15), namely, by $[1-J_0^2(4)]/2\simeq 0.421$ and $|J_0(4)J_2(4)|\simeq 0.145$ for the dc and modulated fluorescence components, respectively.

The solid curve for the dc fluorescence component is identical to Fig. 4 in Shirley's seminal paper,[3] and displays clearly the $N=3$ and $N=5$ multiple quantum resonances. For arbitrary values of $2g/\Omega$ the positions of these resonances, whose deviations from the weak-field values are known as the Bloch-Siegert shifts, may be obtained by any of the methods of Refs. 2–6, or from the theory in Sec. IV of this paper. The results are displayed as the solid curves in Fig. 3 which, in accordance with Eq. (2.15), intersect the $2g/\Omega$ axis at zeros of the zeroth-order Bessel function. The limiting behavior for small interaction strengths, namely, Δ/Ω equals an odd-integer N for the N-quantum resonance, is either explained mathematically by the vanishing of the odd terms a_k from Eq. (2.8) in the zero-damping limit, or is explained physically in terms of N-photon resonances (Fig. 1).

Further inspection of Fig. 2 suggests that the statement

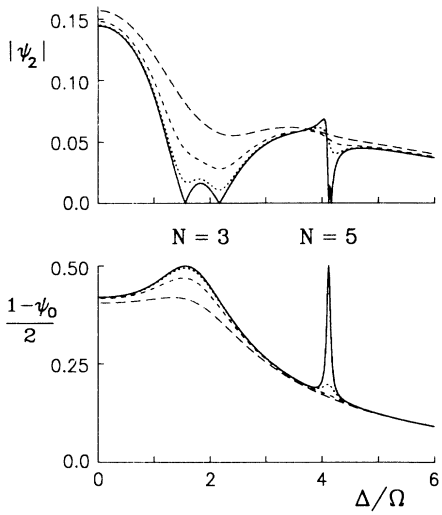

FIG. 2. dc fluorescence (bottom) and amplitude of the fluorescence harmonic at twice the modulation frequency (top) as a function of the scaled detuning, for a fixed Rabi frequency ($2g/\Omega=4$). Solid and dashed curves are for damping rates $\Gamma_u/\Omega=\Gamma_v/\Omega=\Gamma_w/\Omega=10^{-8}$, 0.1, 0.25, and 0.50, respectively. Note the singly and doubly branched structures of the $N=3$ and $N=5$ multiple quantum resonances for the dc and modulated components, respectively.

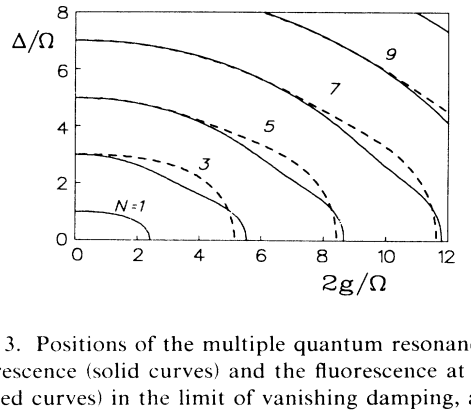

FIG. 3. Positions of the multiple quantum resonances of the dc fluorescence (solid curves) and the fluorescence at 2Ω (solid + dashed curves) in the limit of vanishing damping, as a function of the scaled Rabi frequency and the scaled detuning. The shifts of the dc resonances from the weak-field values are known as Bloch-Siegert shifts. Intersections with the $2g/\Omega$ axis are given by the zeros of the zeroth and second-order Bessel functions.

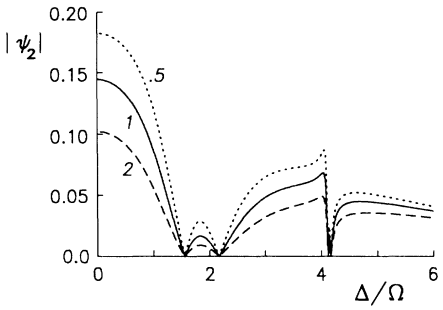

FIG. 4. As Fig. 2 (top). Curves are for $\Gamma_u/\Omega=\Gamma_v/\Omega=10^{-8}$, but different values of the damping ratios Γ_v/Γ_w, as indicated. Note that the values of $|\psi_2|$, but not the positions of its zeros, depend on the ratio Γ_v/Γ_w.

following Eq. (2.15) can be generalized to the case $\Delta\neq 0$. That is, in the limit of vanishing damping, $|\psi_2|$ vanishes if ψ_0 does, so that the dc multiple quantum resonances are present in the modulated component as well. However, $|\psi_2|$ also has additional zeros which, so it appears, can be labeled with the same quantum numbers. Indeed, numerical calculation shows that all multiple quantum resonances of the ψ_2 component are doubly branched, except the $N=1$ resonance. In Fig. 3 the locations of the additional branches are indicated by the dashed curves, which intersect the $2g/\Omega$ axis at zeros of the second-order Bessel function. For small interaction strengths the branches have the same limiting behavior (namely, Δ/Ω = odd N), so that the two parts of any branch are associated with the same quantum number, indeed.

Before deriving the doubly branched structure of the Bloch-Siegert shifts explicitly, we note that, even in the limit of vanishing damping, the values of the Floquet coefficients depend generally on the ratios of the damping terms. This is illustrated for the fluorescence harmonic at 2Ω in Fig. 4, in which the solid curve with $\Gamma_u=\Gamma_v=\Gamma_w=10^{-8}\Omega$ is identical to the upper solid curve from Fig. 2. The other two curves in Fig. 4 are for $\Gamma_u=\Gamma_v=10^{-8}\Omega$, and $\Gamma_v/\Gamma_w=0.5$, and $\Gamma_v/\Gamma_w=2$, respectively. Indeed, the values of $|\psi_2|$ *do* depend on the damping ratio Γ_v/Γ_w. However, the zeros of $|\psi_2|$ seem to be independent of this ratio, a result which we show to be generally valid in Secs. III and IV.

III. VANISHING DAMPING SOLUTION

The theory from Sec. II is well known, although it has been applied only sparingly to the study of modulated interaction components. Neither has it been applied to the study of an ideal atom, namely, one that is undamped and interacts only with (is dressed by) the electromagnetic field. Thus, in this section, we evaluate the Floquet coefficients u_k, v_k, and w_k from Eq. (2.5) in the limit of vanishing damping. That is, we calculate the coefficients

$$z_k^{\mathrm{VDCF}}\equiv\lim_{\Gamma_w\to 0} z_k|_{\gamma_u,\gamma_v},\quad z=u,v,w\ . \tag{3.1}$$

As indicated, the limit is taken for fixed values of the damping ratios $\gamma_u\equiv\Gamma_u/\Gamma_w$ and $\gamma_v\equiv\Gamma_v/\Gamma_w$. Because we obtain this limit from the continued-fraction solution of Eqs.(2.8)–(2.11), we refer to it as the vanishing damping continued-fraction (VDCF) limit. As has been noted by Stenholm[2] one cannot simply set the damping rates in Eq. (2.8) equal to zero, because the continued fractions x_k from Eq. (2.9) would become purely real and the ratio $\mathrm{Im}(x_1)/\Gamma_w$ in Eq. (2.10) would be undetermined. Thus we develop the x_k's to lowest order in the damping Γ_w:

$$x_k=x_k^{(0)}+(i\Gamma_w/g)x_k^{(1)}+O(\Gamma_w^2)\ . \tag{3.2}$$

The factor i/g has been included for notational convenience below. By substituting Eqs. (3.2) and (2.8) into Eq. (2.9) and sorting out terms that are of the same order in the damping, recurrence relations for the $x_k^{(0)}$'s and $x_k^{(1)}$'s are obtained. Of course the $x_k^{(0)}$'s are just the x_k's for zero damping. That is,

$$x_k^{(0)}=(f_k-x_{k+1}^{(0)})^{-1}\ ,\quad k\geq 1 \tag{3.3}$$

with

$$f_k=a_k(\Gamma_u=\Gamma_v=\Gamma_w=0)/ig$$
$$=(k\Omega/g)\times\begin{cases}1-(\Delta/k\Omega)^2, & k=\text{odd}\\ 1, & k=\text{even}\end{cases}\ . \tag{3.4}$$

Having obtained the $x_k^{(0)}$'s, the $x_k^{(1)}$'s follow by recursion of

$$x_k^{(1)}=(x_k^{(0)})^2(g_k+x_{k+1}^{(1)}),\quad k\geq 1 \tag{3.5}$$

where

$$g_k=\begin{cases}\gamma_v+\gamma_u(\Delta/k\Omega)^2, & k=\text{odd}\\ 1, & k=\text{even}\end{cases} \tag{3.6}$$

with γ_u and γ_v as defined following Eq. (3.1). All quantities in Eqs. (3.3)–(3.6) are real. Thus, with Eqs. (2.10) and (3.2), the VDCF result for the dc component becomes

$$\psi_0^{\mathrm{VDCF}}=(1+2x_1^{(1)})^{-1}\ . \tag{3.7}$$

By iteration of Eq.(3.5), $x_1^{(1)}$ can be expressed solely in terms of the $x_k^{(0)}$'s:

$$x_1^{(1)}=\sum_{k=1}^{\infty} g_k p_k^2\ , \tag{3.8}$$

where

$$p_k=\prod_{l=1}^{k} x_l^{(0)}\ . \tag{3.9}$$

Because the g_k's from Eq. (3.6) are non-negative, it follows from Eqs. (3.7)–(3.9) that

$$\psi_0^{\mathrm{VDCF}}\geq 0\ .$$

With Eq. (2.7), ψ_0 is identified as the time-averaged population difference. Thus, in the VDCF limit, a dc popula-

tion inversion of the two-level system is impossible for all values of the interaction strength, detuning, and damping ratios.

With Eqs. (2.11) and (3.9) the VDCF solution for the harmonic components becomes

$$\psi_k^{\mathrm{VDCF}}=p_k\psi_0^{\mathrm{VDCF}},\quad k\geq 1\ . \tag{3.10}$$

Thus, with Eq. (2.7), all nonvanishing coefficients v_k and w_k are determined. The corresponding nonvanishing coefficients u_k are simply found from Eq. (2.6):

$$u_k^{\mathrm{VDCF}}=(\Delta/k\Omega)\psi_k^{\mathrm{VDCF}},\quad k=\text{odd}\ . \tag{3.11}$$

Equations (3.3)–(3.11) constitute the complete VDCF solution. Because all involved quantities are real, an algorithm based on Eqs.(3.3)–(3.6) requires fewer multiplications to compute the Floquet coefficients than the corresponding algorithm from Sec. II, which would involve complex quantities.

For the special case $\Delta=0$ all coefficients f_k from Eq. (3.4) are given by $k\Omega/g$, so that the continued fractions $x_k^{(0)}$ from Eq. (3.3) can be summed analytically:[18]

$$x_k^{(0)}(\Delta=0)=J_k(2g/\Omega)/J_{k-1}(2g/\Omega)\ .$$

Thus, with Eqs. (3.6)–(3.10) and the Bessel-function summation formula[18]

$$\sum_{k=-\infty}^{\infty}(\pm 1)^k J_k^2(x)=J_0(x\mp x)\ ,$$

the VDCF solution for $\Delta=0$ becomes

$$\psi_k^{\mathrm{VDCF}}(\Delta=0)=H^{-1}J_0(2g/\Omega)J_k(2g/\Omega)\ , \tag{3.12}$$

valid for all k. The factor H is given by

$$2H=(1+\gamma_v)+(1-\gamma_v)J_0(4g/\Omega)\ . \tag{3.13}$$

Equations (3.12) and (3.13) are the generalization of Eq. (2.15) for unequal damping rates Γ_v and Γ_w (for $\Gamma_v=\Gamma_w$, i.e., $\gamma_v=1$, $H=1$, as required). Of course the correction term H may also be obtained by a perturbation calculation in terms of $\Gamma_v-\Gamma_w$, using the same analytical technique that originally led to Eqs. (2.14) and (2.15).[12] Because $J_0(4g/\Omega)\leq 1$, the factor H is positive for arbitrary values of $4g/\Omega$ and the ratio γ_v. Thus the zeros of $\psi_k^{\mathrm{VDCF}}(\Delta=0)$ depend on the argument $2g/\Omega$ of the Bessel functions from Eq. (3.12) only and are independent of the damping ratio γ_v, as was established empirically for the zeros of $|\psi_2|$ at the end of Sec. II. For $\Delta=0$ and $2g/\Omega=4$, we calculate $H\simeq 0.793$ for $\gamma_v=0.5$ and $H\simeq 1.414$ for $\gamma_v=2$, thereby correctly predicting the values 0.182 and 0.102 at $\Delta=0$ for the dashed curves in Fig. 4, respectively.

IV. GENERALIZED BLOCH-SIEGERT SHIFTS

Practically speaking, values of the Floquet coefficients calculated from Sec. III are hardly distinguishable from those obtained by substituting extremely small values of the damping rates in the general solution from Sec. II (say, $\Gamma_z\simeq 10^{-8}\Omega$, $z=u,v,w$). However, using the VDCF solution from Sec. III, the resonance behavior of both the dc and the harmonic components is easily analyzed. From Eqs. (3.6)–(3.8) it follows that $\psi_0^{\mathrm{VDCF}}=0$ only if $p_l=\pm\infty$ for at least some $l\geq 1$. For $k\geq 1$ it follows from Eq. (3.10) that $\psi_k^{\mathrm{VDCF}}=0$ if either $\psi_0^{\mathrm{VDCF}}=0$ or $p_k=0$. To establish the vanishing or singularity of the p_k's we note from Eq. (3.3) that if $f_{k+1}=x_{k+2}^{(0)}$ for some k, then $x_{k+1}^{(0)}=\pm\infty$, as a result of which $x_k^{(0)}=0$, but $x_k^{(0)}x_{k+1}^{(0)}=-1$. From this and from Eq. (3.9) it follows that, for $k\geq 1$, $p_k=0$ if, and only if, $x_{k+1}^{(0)}=\pm\infty$, and that $p_k=\pm\infty$ if, and only if, $x_1^{(0)}=\pm\infty$. Combining all the above we conclude that for all $k\geq 0$:

$$\psi_k^{\mathrm{VDCF}}=0\Longleftrightarrow x_1^{(0)}=\pm\infty\ \text{ or }\ x_{k+1}^{(0)}=\pm\infty\ . \tag{4.1}$$

To cast this result into the form most amenable to computing the positions of multiple quantum resonances, we define the quantities $F_k\equiv(g/\Omega)f_k$ and $Y_k\equiv F_{k+1}-(g/\Omega)x_{k+2}^{(0)}$. Thus, with Eq. (3.4),

$$F_k=\begin{cases}k-(\Delta/\Omega)^2/k, & k=\text{odd}\\ k, & k=\text{even}\end{cases} \tag{4.2}$$

and

$$Y_k=F_{k+1}-\cfrac{(g/\Omega)^2}{F_{k+2}-\cfrac{(g/\Omega)^2}{F_{k+3}-\cdots}}\ . \tag{4.3}$$

where Y_k has been written as a continued fraction by iteration of Eq. (3.3). The resonance condition from Eq. (4.1) can now be expressed as

$$\psi_k^{\mathrm{VDCF}}=0\Longleftrightarrow Y_0=0\ \text{ or }\ Y_k=0\ . \tag{4.4}$$

This last result is a generalization of work by Swain in which , in essence, the resonance condition $Y_0=0$ is stated for the dc component of a longitudinally pumped magnetic resonance experiment.[4] With Eqs. (4.2)–(4.4) all information about the positions of multiple quantum resonances can be obtained.

Firstly, because the F_k's from Eq. (4.2) do not depend on the damping ratios γ_u and γ_v, neither do the positions of the resonances, as has already been alluded to in Secs. II and III.

Secondly, Eq. (4.4) implies that the dc component contains only a single set of resonances, namely, those associated with zeros of Y_0. Moreover, these resonances also appear in each of the harmonic components. In turn, each harmonic component ψ_k has an additional set of resonances that are specific to that harmonic, namely, those associated with zeros of Y_k. Thus the doubly branched resonance structure of harmonic components is established.

Thirdly, because, in the weak-field limit, (odd) N-quantum resonances are associated with the vanishing of the corresponding terms F_N from Eq. (4.2) (yielding the resonance conditions $\Delta/\Omega=$odd N) it follows that the term Y_k—and therefore the additional branches of the kth harmonic—contain only those N-quantum resonances for which $N\geq k+1$.

From Eqs. (4.2)–(4.4) the positions of the multiple quantum resonances are easily found by numerical computation. A number of these generalized Bloch-Siegert resonance curves, thusly obtained, are displayed in Fig. 5 (cf. Fig. 3). Branches of the dc component are represented by solid curves. Additional branches of even and odd harmonics, which are associated with the atomic population difference and the atomic susceptibility, are shown in Figs. 5(a) and 5(b), respectively. In all calculations the continued fractions from Eq. (4.3) were truncated at no more than 20 terms. As mentioned under the third property above, additional branches of the kth harmonic are missing for those N-quantum resonances with $N<k+1$. Intersections with the $2g/\Omega$ axis are easily checked to be given by the zeros of the appropriate Bessel functions from Eqs. (2.15) or (3.12). That is, the intersection of the N-quantum resonance of the kth harmonic with the $2g/\Omega$ axis is given by

$$2g/\Omega=\tilde{x}_{kN}=\begin{cases}x_{k,(N-k)/2}, & k=\text{odd}\\ x_{k,(N-k+1)/2}, & k=\text{even}\end{cases} \tag{4.5}$$

where x_{kl} denotes the lth zero of the kth-order Bessel function (not counting the trivial zeros for zero argument). From the asymptotic approximation

$$x_{kl}=(k/2+l-1/4)\pi\ ,$$

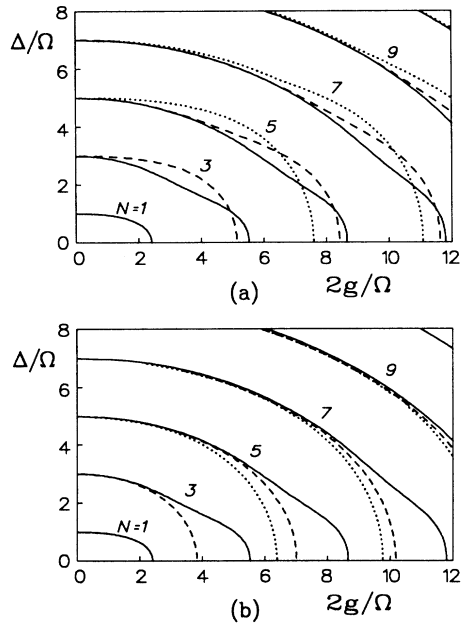

FIG. 5. As Fig. 3: Generalized Bloch-Siegert shifts of the multiple quantum resonances of fluorescence (a) and susceptibility components (b), obtained from Eqs. (4.2)–(4.4). The dc resonances (solid curves) appear also in each of the harmonics. In (a) the dashed and dotted curves represent the additional resonances of the components at 2Ω and 4Ω; in (b) the dashed and dotted curves represent the components at Ω and 3Ω. All intersections with the $2g/\Omega$ axis are given by Bessel zeros, according to Eq. (4.5).

another property of the Bloch-Siegert resonance curves derives, namely, the following.

Fourthly, for an even harmonic the two branches belonging to a certain quantum number converge for large $2g/\Omega$, whereas for an odd harmonic the branches become maximally split. Thus, for odd harmonics, the additional resonances are located midway between the dc-like resonances. Although this property is proved rigorously only from the Bessel function solution for $\Delta=0$, we conclude from Fig. 5 that it is qualitatively correct away from the $2g/\Omega$ axis as well.

From Fig. 5 we draw another tentative conclusion about the Bloch-Siegert resonance curves.

Fifthly, for even harmonics branches belonging to the same quantum number, N are mutually intersecting, whereas the corresponding branches of odd harmonics are nonintersecting, apart from their common origins at $2g/\Omega=0$.

In principle, explicit analytical expressions for the generalized Bloch-Siegert shifts may be obtained from Eqs. (4.2)–(4.4). Specifically, several authors have derived power-series expansions for the dc resonance shifts of a longitudinally pumped magnetic resonance experiment. Thus we expand the position $\Delta_{kN}^{(n)}$ of the (odd) N-quantum resonance of the kth harmonic as

$$\left[\frac{\Delta_{kN}^{(n)}}{\Omega}\right]^2=N^2\left[1+\sum_{m=1}^{n}a_{kN}^{(m)}\left[\frac{g}{2\Omega}\right]^{2m}\right]. \tag{4.6}$$

For an exact result an infinite number of terms n must be included. In practice, as many terms are chosen as the number of expansion coefficients one is willing to evaluate. Rather than the argument $2g/\Omega$, which is used elsewhere in this paper, we have chosen the argument $g/2\Omega$ in Eq. (4.6) because this quantity is equivalent to the scaled Rabi frequency associated with the radio-frequency field in magnetic resonance experiments, usually denoted as b/ω or b/ν. Thus the expansion coefficients $a_{kN}^{(m)}$ may be compared directly with results from the magnetic resonance literature.[2–6] In the Appendix we present an outline for calculating the $a_{kN}^{(m)}$'s. If we introduce the notation

$$\Theta_k^N=\begin{cases}1, & N\geq k\\ 0, & \text{otherwise}\end{cases} \tag{4.7}$$

the results can be written as

$$a_{kN}^{(1)}=-\frac{4}{N}\left[\frac{1}{N+1}\Theta_{k+1}^N+\frac{1}{N-1}\Theta_{k+2}^N\right] \tag{4.8}$$

and

$$a_{kN}^{(2)}=-\frac{4}{N}\left[\frac{N+2}{(N+1)^3}\Theta_{k+1}^N-\frac{N-2}{(N-1)^3}\Theta_{k+3}^N\right]. \tag{4.9}$$

The relative simplicity of these last two results is misleading. Indeed, a laborious calculation shows that the next coefficient is given by

$$a_{kN}^{(3)}=-\frac{4}{N}\left[\frac{(N+2)(N^2+5N+8)}{(N+1)^5(N+3)}\Theta_{k+1}^{N}-\frac{N(N+2)}{(N+1)^4(N-1)}\Theta_{k+2}^{N}-\frac{(N-2)(N^2+N+2)}{(N-1)^5(N+1)}\Theta_{k+3}^{N}+\frac{(N-2)^2}{(N-1)^4(N-3)}\Theta_{k+4}^{N}\right], \tag{4.10}$$

and expressions for higher-order terms will be increasingly complex.

Equations (4.8) and (4.9) agree with expressions for the dc component given by Ahmad and Bullough,[5] who have also given the numerical values $-\frac{21}{16}$, $\frac{173}{1152}$, and $-0.001\,38$ for the third-order coefficients $a_{01}^{(3)}$, $a_{03}^{(3)}$, and $a_{05}^{(3)}$, respectively. These values are easily checked with Eq. (4.10), which identifies the decimally rounded value as $\frac{-43}{31\,104}$. In addition, Ahmad and Bullough have calculated the next-higher terms for the dc main resonance, yielding $a_{01}^{(4)}=-\frac{63}{64}$ and $a_{01}^{(5)}=-\frac{193}{384}$,[5] and Swain has calculated the next-higher term of the $N=3$, dc resonance, yielding $9a_{03}^{(4)}=\frac{4037}{4096}$.[4]

To obtain the positions of the resonances accurately across the entire range (i.e., $0\le 2g/\Omega\le\tilde{x}_{kN}$) the above power-series expansions are of limited use, due to their slow convergence for $g/2\Omega>1$. Indeed, it is generally more convenient to numerically solve for the zeros of the continued fractions Y_k from Eq. (4.3). However, from the structure of Eqs. (4.8)–(4.10), we conclude that, for $k\neq 0$,

$$a_{kN}^{(m)}=a_{0N}^{(m)}\Longleftrightarrow 1\le m\le N-k-1\ . \tag{4.11}$$

Thus $a_{kN}^{(1)}\neq a_{0N}^{(1)}$ only for $N=k+1$. That is, the same Bloch-Siegert shift is displayed by both the dc component and the harmonic components for weak fields, except for the multiple quantum resonances with $N=k+1$. Note that this latter exception was not made by Arimondo and Moruzzi in their discussion of the harmonic signal at twice the modulation frequency in a longitudinally pumped magnetic resonance experiment[7] (see the quotation at the end of the second paragraph in Sec. I of this paper). It is easily checked in Fig. 3 and in Fig. 5(a) that the additional $N=3$ and $N=5$ resonances of the fluorescence harmonics at 2Ω and 4Ω indeed deviate from the dc-like resonances for even small values of $2g/\Omega$. More generally it follows from Eq. (4.11) that the larger the difference $N-k$, the less the additional resonances deviate from the corresponding dc-like resonances. For example, the $N=3$, $N=5$, and $N=7$ additional resonances of the fluorescence harmonic at 2Ω deviate from the dc-like resonance by less than 0.01 (i.e., $|\Delta_{2N}-\Delta_{0N}|/\Omega<0.01$) for $2g/\Omega\le 0.40$, 3.13, and 6.13, respectively.

Analytical expressions for the (dc) Bloch-Siegert shifts in magnetic resonance experiments other than power-series expansions have been derived, namely, expressions in terms of rational fractions,[4] and Bessel-function solutions for small but nonzero detuning (or rather, small but nonzero Zeeman fields).[4–6] Although similar expressions might be derived for the additional resonances of harmonic components, we contend that numerically solving Eqs. (4.2)–(4.4) is sufficiently easy and efficient for all practical purposes.

V. DISCUSSION AND CONCLUSION

We have shown that, for sufficiently small damping, the modulated interaction components of a two-level atom driven by a FAM field display not only the resonances that are found in the time-averaged fluorescence signal, but also additional resonances that are specific to the harmonic component. However, as shown in Fig. 2, this doubly branched resonance structure is easily obscured by relaxation effects. Thus, to verify this effect experimentally, one must employ a modulation frequency that is sufficiently large to overcome the loss of coherence due to spontaneous emission or other mechanisms.

To establish a quantitative criterion for the observability of the doubly branched resonances, we have computed the zeros of the real parts of the Floquet coefficients ψ_1 and ψ_2, which correspond to the quadrature component of the imaginary part of the susceptibility at Ω and the in-phase fluorescence component at 2Ω, respectively. The positions of the zeros of the $N=1$ and $N=3$ resonances, which were calculated using the general theory of Sec. II, are displayed in Fig. 6. Radiative damping has been assumed (i.e., $\Gamma_u=\Gamma_v=\Gamma_w/2\equiv 1/T_2$), and the curves are labeled with the value of $(\Omega T_2)^{-1}$. As can be seen from the solid curves, the lower and upper lobes of the $N=3$ resonance of the fluorescence component at 2Ω disappear for $(\Omega T_2)^{-1}\simeq 0.075$ and $(\Omega T_2)^{-1}\simeq 0.175$, respectively. By contrast, the structure of the susceptibility component at Ω (dashed curves) is preserved for relatively large damping rates, although, for $(\Omega T_2)^{-1}\simeq 0.45$, the

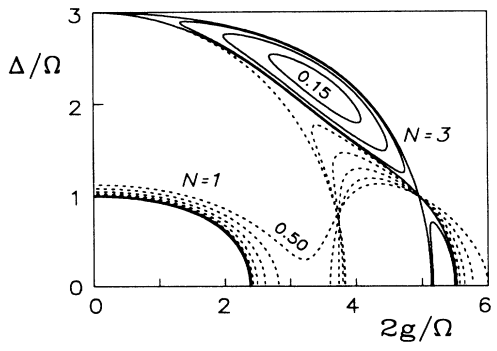

FIG. 6. Zeros of $\mathrm{Re}(\psi_1)$ (dashed curves) and of $\mathrm{Re}(\psi_2)$ (solid curves) for $T_1/T_2=0.5$ and various values of the product $(\Omega T_2)^{-1}$ [see Eqs. (2.1)]. Solid curves correspond to the in-phase component of the fluorescence at 2Ω for $(\Omega T_2)^{-1}=0.00$, 0.05, 0.10, and 0.15. Dashed curves correspond to the quadrature component of the imaginary part of the susceptibility at Ω for $(\Omega T_2)^{-1}=$ 0.0, 0.1, 0.2, 0.3, 0.4, and 0.5.

$N=1$ and $N=3$ branches merge. This means that in an experiment like that of Chakmakjian *et al.* a modulation frequency of some 100 MHz should be employed to resolve the doubly branched structure of the $N=3$ resonance in the modulated fluorescence signal from the sodium D_2 line.[11]

The only relevant experimental work, known to us, in which a modulated interaction component is measured rather than a dc signal is that of Arimondo and Moruzzi. These authors have measured the population difference at twice the modulation frequency in a longitudinally pumped magnetic resonance experiment involving an optically pumped ^{199}Hg vapor.[7] Although different resonance behaviors for the modulated and dc signals are found, evidence for a doubly branched resonance structure is precluded due to too small a modulation frequency [i.e., too large a value of $(\Omega T_2)^{-1}$]. Technically speaking, employing a larger modulation frequency would perhaps have been easier in these magnetic resonance experiments than it will be in the ongoing work on optical resonance. However, it seems not to have been realized at the time just how the resonance behavior of modulated interaction components differs from that of the dc component, so that no exhaustive investigation was conducted.

As we have argued recently,[14] the doubly branched resonance structure of harmonic components significantly pronounces their resonance behavior over that of the dc component, even if the doubly branched structure itself is obscured in the presence of damping. As a result, the modulated components, unlike the dc component, should retain significant resonance structure even in the case of a strongly inhomogeneously broadened medium.[14] Thus experimental observation of this inhomogeneously broadened resonance behavior of harmonic components would constitute indirect support for the theory presented in this paper.

Finally we remark that a similar treatment can be given for the excitation of a two-level system by a not-fully-amplitude-modulated field,[9,19,20] a frequency-modulated field,[21,20] or a bichromatic field with unequal intensities in the two modes,[22] each of which also has analogues in magnetic resonance. We hope to present this work in future publications.

ACKNOWLEDGMENTS

This work was supported by the "Centers of Excellence" program of the State of Tennessee and by the U.S. Army Research Office.

APPENDIX

In this appendix we present a concise outline of the derivation of the power-series expansions of the Bloch-Siegert shifts as given in Eqs. (4.6)–(4.10). For convenience we introduce the variables $x\equiv-(g/\Omega)^2$ and $y\equiv(\Delta_{kN}/\Omega)^2$. Also, we rescale the coefficients from Eq. (4.6) according to

$$\alpha_m\equiv -Na_{kN}^{(m)}/(-4)^m\ . \tag{A1}$$

Substituting Eq. (4.6) into Eq. (4.2) yields a power-series expansion for the terms F_n (we reserve the indices N and k for the Nth resonance of the kth harmonic):

$$F_n\equiv\sum_{m=0}^{\infty}F_n^{(m)}x^m\ , \tag{A2}$$

where

$$F_n^{(0)}=\begin{cases}n-N^2/n, & n=\text{odd}\\ n, & n=\text{even}\end{cases} \tag{A3a}$$

and, for $m>0$,

$$F_n^{(m)}=\begin{cases}(N/n)\alpha_m, & n=\text{odd}\\ 0, & n=\text{even}\end{cases}\ . \tag{A3b}$$

Subsequently we write the continued fraction Y_k from Eq. (4.3)—truncated after n divisions—as a single fraction with numerator A_n. The numerators A_n satisfy the recurrence relation[23]

$$A_n=F_{k+n+1}A_{n-1}+xA_{n-2},\quad n\geq 0\ , \tag{A4a}$$

with

$$A_{-1}=1,\quad A_n=0\ \text{ for } n<-1\ . \tag{A4b}$$

Expanding the A_n's as a power series (dropping the subscripts N and k):

$$A_{N-k+n}\equiv\sum_{m=0}^{\infty}A_n^{(m)}x^m \tag{A5}$$

and substituting Eq. (A2), this leads to the following recurrence relations, valid for $n\geq k-N$:

$$A_n^{(0)}=F_{N+n+1}^{(0)}A_{n-1}^{(0)}\ , \tag{A6a}$$

and, for $m>0$,

$$A_n^{(m)}=A_{n-2}^{(m-1)}+\sum_{l=0}^{m}F_{N+n+1}^{(l)}A_{n-1}^{(m-1)}\ . \tag{A6b}$$

To satisfy the condition $Y_k=0$ from Eq. (4.4), we must require that $A_{\infty}^{(m)}=0$ for all $m\geq 0$. This can be accomplished by requiring that

$$\lim_{n\to\infty}\{A_n^{(m)}\}=0\ \text{ for all } 0\leq m\leq n+1\ . \tag{A7}$$

Because, from Eq. (A3a), $F_N^{(0)}=0$, it follows from Eq. (A6a) that $A_n^{(0)}=0$ for all $n\geq -1$. From Eq. (A6b), it then follows that $A_n^{(m)}=0$ for all $n>m-1$, *if* one imposes the condition

$$\left[A_{m-1}^{(m)}=0\right]\Longrightarrow\alpha_m,\quad m=1,2,3,\ldots\ . \tag{A8}$$

Thus Eq. (A7) is satisfied indeed. As is indicated, solving Eq. (A8) renders successively the desired coefficients α_m.

As an illustration we calculate the first coefficient α_1. By iterating Eq. (A6b) and using Eqs. (A3) we obtain

$$A_0^{(1)}=A_{-2}^{(0)}+(N+1)\left[A_{-3}^{(0)}+\alpha_1A_{-2}^{(0)}\right]\ . \tag{A9}$$

From Eq. (A6) it can be shown that

$$A^{(0)}_{-p}/A^{(0)}_{-2}=\Theta^{N}_{k+p-1}\Big/\prod_{q=1}^{p-2}F^{(0)}_{N-q},\quad p\geq 2 \tag{A10}$$

with Θ as defined in Eq. (4.7). Substituting Eq. (A10) into Eq. (A9) and requiring that $A^{(1)}_{0}=0$ then yields α_1 and, with Eq. (A1), the first-order term of the Bloch-Siegert shift as given in Eq. (4.8).

Higher-order terms are obtained in a similar fashion. In order to eliminate terms $A^{(m)}_{n}$ with $m>0$, we have used the expressions

$$A^{(0)}_{-3}A^{(1)}_{-2}-A^{(1)}_{-3}A^{(0)}_{-2}=A^{(0)}_{-3}A^{(0)}_{-4} \tag{A11}$$

to obtain α_2 and, in addition to Eq. (A11), the expression

$$A^{(0)}_{-4}A^{(1)}_{-2}-A^{(1)}_{-4}A^{(0)}_{-2}=A^{(0)}_{-4}[A^{(0)}_{-4}+(N-1)(F^{(1)}_{N-2}A^{(0)}_{-4}+A^{(0)}_{-5})] \tag{A12}$$

to obtain α_3. Equations (A11) and (A12) can be derived from Eqs. (A3) and (A5).

It would seem feasible to write an algorithm based on Eqs. (A3), (A6), (A8), and (A10) by which arbitrarily high-order coefficients α_m can be computed. Although we have given this approach some thought, we have been unable to come up with such an algorithm, mainly because of the difficulty of generalizing the implementation of expressions like Eqs. (A11) and (A12).

[1] J. Margerie and J. Brossel, C. R. Acad. Sci. **241**, 373 (1955); J. M. Winter, *ibid.* **241**, 375 (1955); Ann. Phys. (Paris) **4**, 745 (1959).

[2] S. Stenholm, J. Phys. B **5**, 878 (1972); **5**, 890 (1972); **6**, L240 (1973).

[3] J. H. Shirley, Phys. Rev. **138**, B979 (1965).

[4] S. Swain, J. Phys. B **7**, 2363 (1974).

[5] F. Ahmad and R. K. Bullough, J. Phys. B **7**, L147 (1974); **7**, L275 (1974).

[6] C. S. Chang and P. Stehle, Phys. Rev. A **4**, 641 (1971); D. T. Pegg, J. Phys. B **6**, 241 (1973); C. Cohen-Tannoudji, J. Dupont-Roc, and C. Fabre, *ibid.* **6**, L214 (1973); **6**, L218 (1973); P. Hannaford, D. T. Pegg, and G. W Series, *ibid.* **6**, L222 (1973).

[7] E. Arimondo and G. Moruzzi, J. Phys. B **6**, 2382 (1973).

[8] S. Feneuille, M.-G. Schweighofer, and G. Oliver, J. Phys. B **9**, 2003 (1976).

[9] P. Thomann, J. Phys. B **9**, 2411 (1976); **13**, 1111 (1980); B. Blind, P. R. Fontana, and P. Thomann, *ibid.* **13**, 2717 (1980).

[10] L. W. Hillman, J. Krasinski, R. W. Boyd, and C. R. Stroud, Jr., Phys. Rev. Lett. **52**, 1605 (1984); L. W. Hillman, J. Krasinski, K. Koch, and C. R. Stroud, Jr., J. Opt. Soc. Am. B **2**, 211 (1985).

[11] S. Chakmakjian, K. Koch, and C. R. Stroud, Jr., J. Opt. Soc. Am. B **5**, 2015 (1988).

[12] Actually, the interpretation of subharmonic resonances as the limiting behavior of multiple quantum resonances is not given in Refs. 10 and 11. Also, in Ref. 11 an empirical expression for the positions of the dc subharmonic resonances is given. For a discussion, see W. M. Ruyten, J. Opt. Soc. Am. B (to be published).

[13] D. Keefer, Appl. Opt. **26**, 91 (1987); W. M. Ruyten, L. M. Davis, C. Parigger, and D. R. Keefer, in *Advances in Laser Science-III,* edited by A. C. Tam, J. L. Gole, and W. C. Stwalley (AIP, New York, 1988), pp. 155–157; L. M. Davis, Phys. Rev. Lett. **60**, 1258 (1988).

[14] W. M. Ruyten, *Optical Society of America Annual Meeting,* Vol. 11 of the *1988 Technical Digest Series* (Optical Society of America, Washington, D.C, 1988), p. 63; W. M. Ruyten, Opt. Lett. **14**, 506 (1989).

[15] L. Allen and J. H. Eberly, *Optical Resonance and Two-Level Atoms* (Wiley, New York, 1975), Sec. 3.4.

[16] With these choices the vanishing damping expressions for the combined Floquet coefficients ψ_k from Eq. (2.7) do not have to differentiate between odd and even indices [cf. Eqs. (2.15), (3.10), and (3.12)].

[17] S. Stenholm and W. E. Lamb, Jr., Phys. Rev. **181**, 618 (1969).

[18] *Handbook of Mathematical Functions,* edited by M. Abramowitz and I. A. Stegun (Dover, New York, 1972), Sec. 9.1.

[19] G. S. Agarwal and N. Nayak, J. Phys. B **19**, 3385 (1986).

[20] W. M. Ruyten, Phys. Rev. A **39**, 442 (1989).

[21] N. Nayak and G. S. Agarwal, Phys. Rev. A **31**, 3175 (1985).

[22] G. S. Agarwal and N. Nayak, J. Opt. Soc. Am. B **1**, 164 (1984).

[23] W. H. Press and S. A. Teukolsky, Comput. Phys. **2**(5), 88 (1988).